Journal of Engineering Mathematics **40:** 399–411, 2001.

Moving phreatic surface in a porous slab: an analytical solution

A. R. KACIMOV and N. D. YAKIMOV[1]
Department of Soil & Water Sciences, P.O. Box 34, Al-Khod 123, Sultan Qaboos University, Sultanate of Oman (E-mail: anvar@squ.edu.om)
[1]*Institute of Mathematics and Mechanics, Kazan University, 17, University Str., Kazan, 420008, Tatarstan, Russia*

Received 7 March 2000; accepted in revised form 19 February 2001

Abstract. Transient Darcian flow in an inclined rigid fully saturated porous layer is studied. A phreatic surface of fixed shape driven by uniformly increasing (but generally not equal) water levels in the contiguous reservoirs moves upward with a constant velocity. In a system of coordinates travelling with the reservoir water level the real and imaginary parts of the complex potential (an analytic function) and complex coordinate are linearly interconnected along the boundary of the flow domain that allows implementing the Polubarinova-Kochina method. An explicit analytic equation of the free surface is derived and shown to result in non-trivial configurations including the saturated zone overhanging dry areas.

Key words: complex potential, free surface, hodograph, Polubarinova–Kochina, porous media.

1. Introduction

A phreatic surface or water table is the interface between the saturated and unsaturated zone in aquifers and hydrotechnic constructions (dams, embankments, liners, to name few). Mathematically this surface is a free boundary, along which two conditions hold, a dynamic condition (isobaricity) and a kinematic condition requiring that all front particles stay with the front wherever it moves. Determination of this free surface is a daunting nonlinear problem, which is often circumvented through hydraulic approximations (the Dupuit-Forchheimer model), linearizations (the linear potential model), or a simple ignorance of the flow transience in steady-state models (*e.g.* [1–8]). However, in some cases high-amplitude fluctuations of water levels occur and seepage is not dominantly horizontal (for example, flow through an embankment exposed to flood-type variations of the head and tail water levels) and, hence, one has to use the nonlinear potential model [1, pp. 547–550].

Due to analogies with other free-boundary problems [9–10], the phreatic-surface problem has attracted considerable attention of applied mathematicians [11–13]. There are still very few simple analytic solutions in terms of the full nonlinear model, which could verify practical calculations based on numerical codes.

In this paper we develop a new, simple but rigorous solution for an advancing phreatic-surface problem. We consider a 2-D flow in a porous slab where a free surface is 'pulled' up by increasing water levels in adjacent reservoirs. In a moving coordinate system the configuration of the free surface is stationary, *i.e.*, we have a travelling-wave solution. The head distribution is governed by the Laplace equation and transient features appear due to variations of the head along the reservoir boundaries.

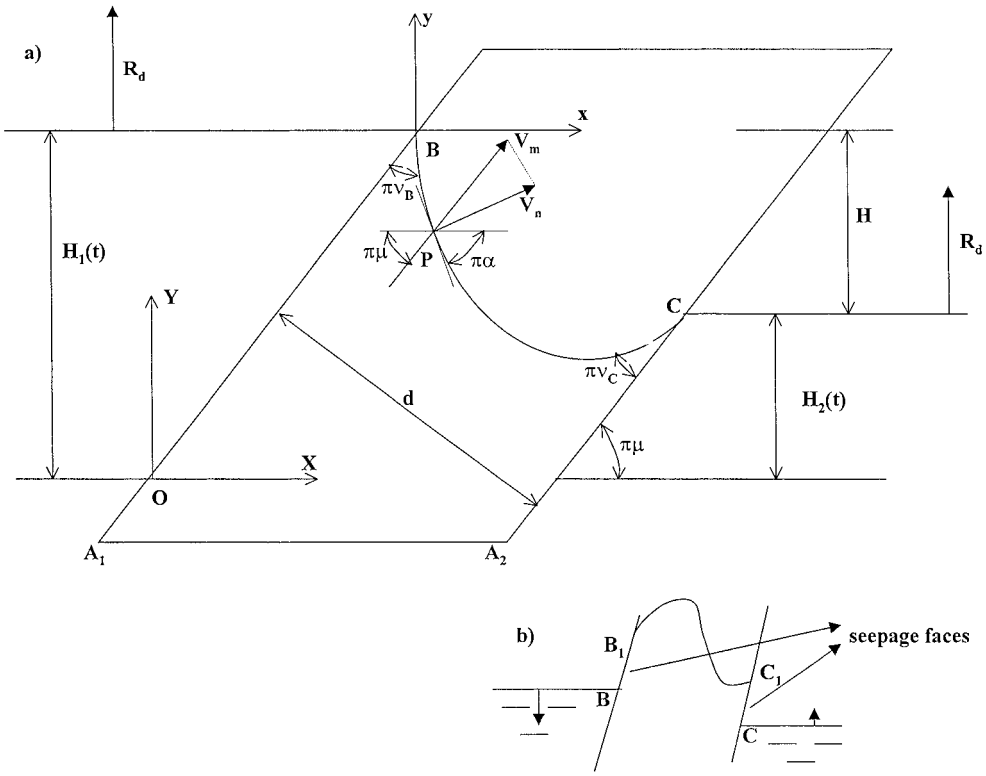

Figure 1. Flow in a tilted layer.

2. Mathematical model

We consider a tilted homogeneous porous layer of constant thickness d, conductivity k, and porosity m (Figure 1a). The angle of inclination is $\pi\mu$, $0 < \mu < \frac{1}{2}$. The layer separates two reservoirs, in which the water level rises with a rate R_d. The hydraulic head loss across the layer, H, remains constant. A free surface BC advances within the layer. Figure 1a and all further figures show the case when the hydraulic head along A_1B is higher than along A_2C, though reverse-flow regimes are possible.

We consider both the soil and water as incompressible, seepage as Darcian, the layer as homogeneous and isotropic. We neglect the capillary fringe and the unsaturated zone and assume that BC separates completely wet and dry zones.

The hydraulic head h_i along the left (A_1B) and right (A_2C) boundaries is $h_i = H_1(t)$ and $h_i = H_2(t)$ (t is time), *i.e.*, AC and AB are equipotential boundaries. The head is counted from an arbitrary datum level OX.

For simplicity, we restrict ourselves to the flow regimes, for which the reservoir levels and the free surface coincide at points B and C. For arbitrary $H_1(t)$ and $H_2(t)$ it is not the case and seepage faces (BB_1 and CC_1 in Figure 1b) may appear (so-called decoupling [7]). Therefore, to avoid the seepage faces we assume that H is not too high (in particular, $H = 0$ is allowable). We shall derive explicitly the restriction on H, which guaranties no decoupling.

Thus, the water levels H_1 and H_2 increase uniformly and synchronically as

$$H_1 = R_d t + H, \qquad H_2 = R_d t, \tag{1}$$

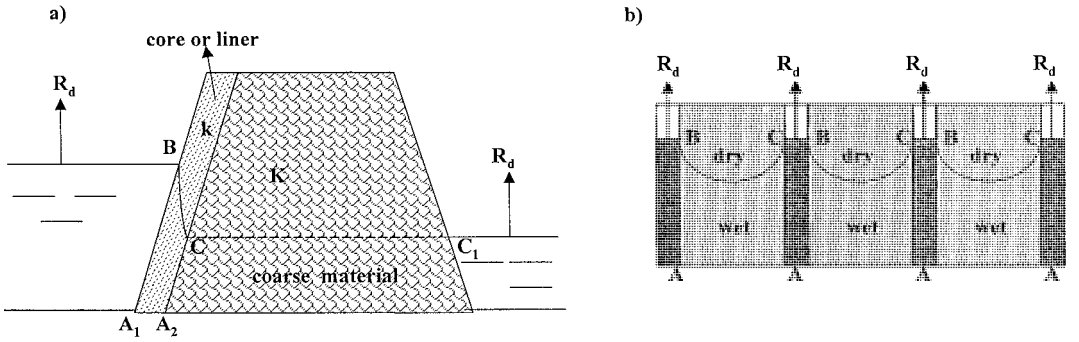

Figure 2. Physical systems with advancing phreatic surfaces: a dam (a), a composition of fractures and blocks (b).

where R_d is a constant rate, which can be found from the ascending limb of the corresponding hydrograph, H is the constant head difference between A_1B and A_2C.

In cheap embankments designed to sustain low H values the bulk dam volume is made up of a coarse material (say, gravel) of high conductivity K and only thin clay liner or core of low conductivity k is constructed (Figure 2a). Then, the phreatic surface in the coarse filling is a straight (dashed in Figure 2a) line CC_1 [14, p. 233]. Any variations of the tail water level induce a fast response of CC_1, which remains nearly straight. Hence, at $K \gg k$ the coarse part can be disregarded and flow in the liner as in Figure 1a should be studied. Another justification of the scheme in Figure 1a can be found in geomechanics. In fractured media (Figure 2b) water can quickly rise in the constituting system of fractures, while porous blocks of a relatively lower permeability are wetted slowly. Usually, capillarity plays a crucial role in the process of imbibition into blocks. However, we shall show that, even in purely gravity-driven flows there always exists nonuniformity of wetting caused by a non-flat phreatic surface, which lags behind the fracture water level as in Figure 2b.

The layer in Figure 1a is not restricted from below, *i.e.*, we neglect the impermeable bottom as in Figure 2a (or any other boundaries) far behind the free surface. We consider the process of water rise after sufficient time such that BC is stabilized and moves along the layer without shape changes (so-called traveling wave regime). The velocity of this movement is:

$$V_m = R_d / \sin \mu. \tag{2}$$

A snapshot flow picture is shown in Figure 3a. Far enough from the free surface (near A_1 and A_2) the flow is nearly steady and nearly one-dimensional. The velocity here equals kH/d and is perpendicular to A_1B and A_2C. Near the advancing front seepage is 2-D. In particular, there exists a hinge point M on A_2C. It means that water flows into the down pool from the slab through A_2M and from the reservoir into the layer – through MC. Clearly, a particle which has moved into the layer from MC is finally forced to come back into the down pool, *i.e.*, its trajectory makes a loop.

For mathematical convenience (similarly to the Saffman-Taylor viscous fingering problem [9]), we adopt the moving coordinates (xBy), which origin B travels along the right-hand boundary of the flow domain, *i.e.*

$$x = X - R_d \cot \mu t, \qquad y = Y - R_d t, \tag{3}$$

where X, Y are space-fixed coordinates. Owing to this change the value of hydraulic head becomes:

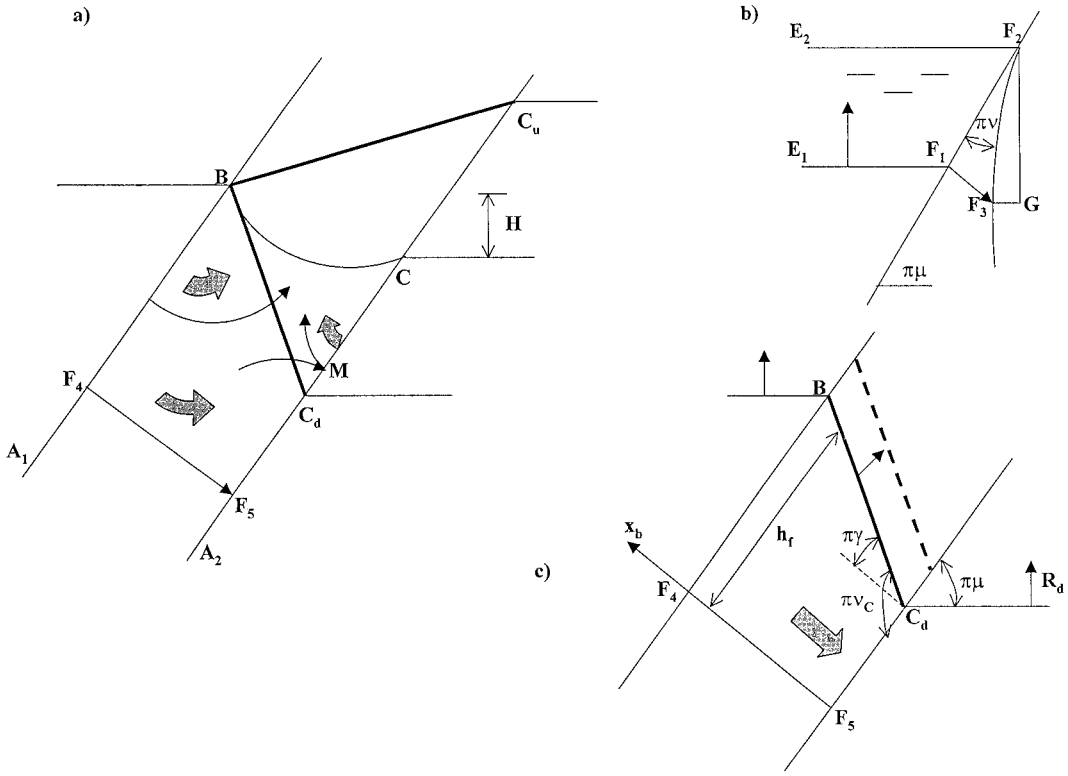

Figure 3. Instantaneous streamline picture with the ultimate straight free surfaces (a), flow picture near the free surface -reservoir contact (b), travelling-wave solution to the Bousinesq model (c).

$$h = h_i - R_d t. \tag{4}$$

The head $h_i(x, y, t)$ is a harmonic function within the layer (recall the incompressibility assumption) and so is the transformed head

$$\Delta h(x, y) = 0 \tag{5}$$

with boundary conditions derived from (1) and (4):

$$h = H \quad \text{along} \quad AB, \qquad h = 0 \quad \text{along} \quad AC. \tag{6}$$

Along the free surface BC a standard isobaric condition holds $h_i = Y$ or

$$h = y. \tag{7}$$

From elementary trigonometry, at any point P on the free surface (Figure 1a) $V_m = V_n(s)/\sin[\alpha(s) + \mu]$, where V_n is the position-dependent propagation velocity of the free surface in the direction along the outer normal to BC, s is the arc coordinate along BC, and $\alpha(s)$ is the angle between BC and the horizontal level (Bx). From the Darcy law we have:

$$V_n = -\frac{k}{m}\frac{\partial h}{\partial n}.$$

Combining this expression with the kinematic condition (2) we arrive at

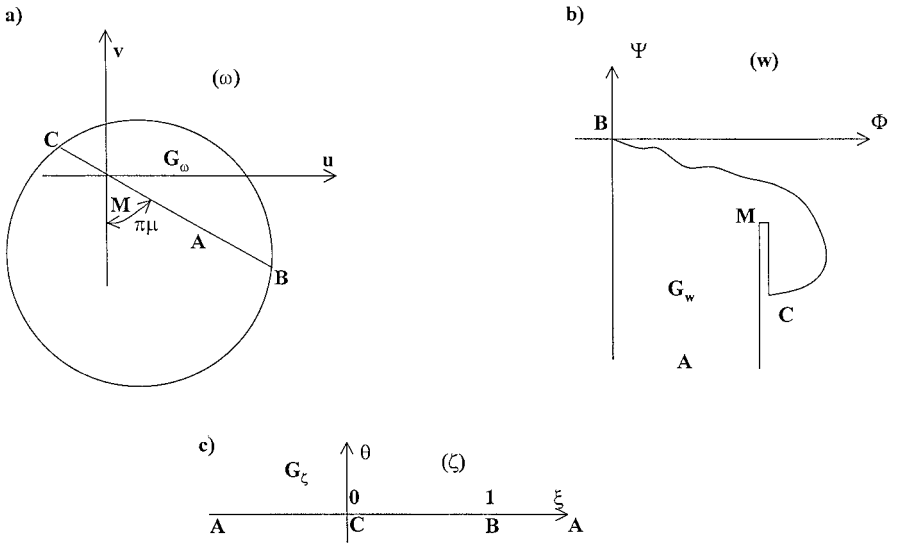

Figure 4. Hodograph (a), the complex-potential domain (b), and an auxiliary plane (c).

$$\frac{\partial h}{\partial n} = R\frac{\sin(\alpha+\mu)}{\sin\mu}, \tag{8}$$

where $R = mR_d/k$ is a non-dimensional rate of rise.

Thus, (3) transforms XOY to xBy and the moving boundary-value problem is reduced to the determination of a harmonic function (5) with boundary conditions (6–8) in a time-independent domain with *a priori* unknown BC.

3. Solution

3.1. Statement of the boundary-value problem

We introduce the complex coordinate $z = x + \mathrm{i}y$, the complex potential $w = \Phi(x, y) + \mathrm{i}\Psi(x, y)$ where $\Phi = -kh$ is the velocity potential and Ψ is the stream function, and the complex hodograph $\omega = u + \mathrm{i}v$. We designate the flow domain as G_z and the corresponding domains in ω-plane and w-plane as G_ω and G_w, respectively. The functions $w(z)$ and $u - \mathrm{i}v = \mathrm{d}w/\mathrm{d}z$ are analytic within G_z. The domain G_ω is shown in Figure 4a. Clearly, points A_1 and A_2 in G_ω coincide and are represented by one point A. The domain G_w is diagrammed in Figure 4b (we assume $\Psi_B = 0$). There is a cut in G_w because BC is not monotonic with respect to Φ. It reflects the fact that water flows from MC into the slab.

Along each part of the boundary of G_z a pair of linear conditions is satisfied:

$$\begin{aligned}
&\Phi = kH, && x\sin\pi\mu - y\cos\pi\mu = 0 && \text{along} \quad AC,\\
&\Phi = 0, && x\sin\pi\mu - y\cos\pi\mu + d = 0 && \text{along} \quad AB,\\
&\Phi + ky = 0, && \Psi + kR(x - y\cot\pi\mu) = 0 && \text{along} \quad BC.
\end{aligned} \tag{9}$$

The second condition along BC in (9) follows directly from (8) upon substitution of the obvious equalities

$$\frac{\partial h}{\partial n} = \frac{1}{k}\frac{\partial\Psi}{\partial s}, \qquad \cos\alpha = -\frac{\mathrm{d}x}{\mathrm{d}s}, \qquad \sin\alpha = \frac{\mathrm{d}y}{\mathrm{d}s}$$

in (9) and integration with respect to s. Note, that the pair of conditions along BC is equivalent to the Polubarinova–Kochina [1, p. 340] conditions along a steady phreatic surface with a distributed infiltration-evaporation, the intensity of which depends on *two* Cartesian coordinates (in standard models of accretion along the water table Ψ is assumed to be a function of x [1, p. 51, 15]). Hence, the circle, whose segment corresponds to BC in G_ω, is not centered at the ordinate axis as in the case of phreatic surfaces with x-dependent accretion or in equivalent problems with a salt-fresh water sharp interface where $\Phi - cy = 0$, $\Psi = 0$ [1, pp. 330–340].

We introduce an auxiliary variable $\zeta = \xi + \mathrm{i}\theta$ depicted in Figure 4c and map G_w and G_z onto the upper half-plane of ζ, G_ζ. According to the Riemann theorem the correspondence between three boundary points in G_z and G_ζ can be selected arbitrarily and we choose them as is shown in Figure 4c.

To reconstruct the analytic function $z(\zeta)$, we employ the Polubarinova–Kochina method [1, pp. 240–264], which has been recently applied to several free-boundary problems [15–18]. We use two functions $Z(\zeta) = \mathrm{d}z/\mathrm{d}\zeta$ and $W(\zeta) = \mathrm{d}w/\mathrm{d}\zeta$ which make conditions (9) homogeneoues [1].

The points A, B, C where the boundary conditions (9) change are called singular points. We have to examine the behavior of Z and W (which we both designate as f) at these points.

First, we determine the angles $\pi\nu_B$ and $\pi\nu_C$ between BC and the reservoir boundaries (Figure 1a). Unlike the Polubarinova-Kochina analysis in steady regimes, we have to take into account the transience. We consider a small time step $\mathrm{d}t$ during which the water level in the pools increases from E_1F_1 to E_2F_2 (Figure 3b, F_2 corresponds to either B or C in Figure 1a). The free surface advances near the 'tip' F_2 in such a way that the segment F_2F_3 can be approximated as a straight line. Seepage near this tip is nearly one-dimensional and perpendicular to the pool boundary F_1F_2. During this time lapse a marked water particle moves from point F_1 ($t = 0$) at the reservoir bed to point F_3 ($t = \mathrm{d}t$) within the slab. The distance passed is $|F_1F_3| = V_{F_1}\,\mathrm{d}t$. Obviously, $|F_1F_2| = R_d\mathrm{d}t/\sin\pi\mu$. Hence,

$$\tan\pi\nu = \frac{|F_1F_3|}{|F_1F_2|} = \frac{V_{F_1}}{R_d}\sin\pi\mu. \tag{10}$$

Directly from the Darcy law (one-dimensional flow)

$$V_{F_1} = \frac{k}{m}\frac{\mathrm{d}h}{|F_1F_3|}, \tag{11}$$

where $\mathrm{d}h$ is the head difference between points F_1 and F_3. Counting the head from E_2F_2 we can write $\mathrm{d}h = |F_2G| = |F_2F_3|\cos\pi(\frac{1}{2} - \mu - \nu)$. Because $|F_1F_3| = |F_2F_3|\sin\pi\nu$, we combine (10) and (11) in

$$R\tan\pi\nu = \sin\pi\mu\frac{\sin\pi(\mu+\nu)}{\sin\pi\nu},$$

which is reduced to a quadratic equation with respect to $\cot\pi\nu$:

$$\cot^2\pi\nu + \cot\pi\mu\ \cot\pi\nu - \frac{R}{\sin^2\pi\mu} = 0.$$

Its solution yields two roots, *i.e.*, the angles (Figure 1a) are

$$\begin{aligned}\nu_B &= \frac{1}{\pi}\mathrm{arccot}\frac{\sqrt{\cos^2\pi\mu + 4R} - \cos\pi\mu}{2\sin\pi\mu},\\ \nu_C &= \frac{1}{\pi}\mathrm{arccot}\frac{\sqrt{\cos^2\pi\mu + 4R} + \cos\pi\mu}{2\sin\pi\mu}\end{aligned} \tag{12}$$

where $0 < \nu_C < \mu$ and $0 < \nu_B < 0{\cdot}5$.

3.2. Reconstruction of characteristic function

Using the Polubarinova-Kochina technique we could have introduced the determinants, calculated the exponents near the singular points, written out the Riemann P-function, and arrived at a pair of linearly independent solutions of the corresponding Fuchsian equation in terms of the hypergeometric function (with different representation near the three points). However, we shall use an alternative form of the Polubarinova–Kochina method without resorting to the theory of ordinary differential equations.

The functions $f(\zeta)$ to be found constitute a set with the following properties:

3.2.1. *Property 1*

$f(\zeta)$ are analytic including the boundary of G_ζ, except for the three singular points $\zeta_i,\ i = 3$. Hence, through any part of the real axis $C\xi$ between two neighboring singular points the functions can be continued from G_ζ to the lower half-plane $\Im(\zeta) < 0$. In the vicinity of the singular points f may be written as [16]:

$$f(\zeta) = (\zeta - \zeta_i)^{\beta_i}\Phi_{1i}(\zeta) + (\zeta - \zeta_i)^{\beta_i+\gamma_i}\Phi_{2i}(\zeta), \tag{13}$$

where $\Phi_{1i}(\zeta)$ and $\Phi_{2i}(\zeta)$ are analytic in the vicinity of ζ_i, *i.e.*, in the disks $|\zeta| < 1$, $|\zeta - 1| < 1$ and $\zeta > 1$, $\zeta < 0$; the constants β_i and γ_i ($\gamma_i > 0$) are the same for all functions from the set. The singular points ζ_i and parameters β_i, γ_i defining this class are determined from (9).

3.2.2. *Property 2*

If one chooses two different (linearly independent) functions from the set, then any function from the set can be represented as a linear combination of these two functions. In other words, the class is two-parametric and any function from the set is defined by ζ_i, β_i, γ_i up to two complex constants.

3.2.3. *Property 3*

If the domains G_z and G_w are infinite strips with parallel boundaries in the vicinity of a singular point $\zeta_j = \infty$, then f can be represented near ζ_j as

$$f(\zeta) = \frac{\Phi(\zeta)}{\zeta - \zeta_j}.$$

The analytic function $\Phi(\zeta)$ is not zero at this point. Then this singular point is called a removable singularity.

In our problem, $z(\zeta)$, $w(\zeta) \sim \log\zeta$ near A and hence A is a removable singularity. Two essentially singular points are C and B. This reduces the solution for Z to elementary functions instead of hypergeometric functions in the general case of three non-removable singularities.

According to *Property 1* and (13), the functions $f(\zeta)$ can be represented near $\zeta = 0$ as

$$f(\zeta) = \zeta^{\beta_C}[\Phi_{C1}(\zeta) + \zeta^{\gamma_C}\Phi_{C2}(\zeta)].$$

The functions $\Phi_{C1}(\zeta)$ and $\Phi_{C2}(\zeta)$ are analytic in the whole plane, except for $\zeta = 1$, *i.e.*, can be written as:

$$\Phi_{C1}(\zeta) = (\zeta - 1)^{\beta_B}\left[\Phi_{11}(\zeta) + (\zeta - 1)^{\gamma_B}\Phi_{12}(\zeta)\right],$$

$$\Phi_{C2}(\zeta) = (\zeta - 1)^{\beta_B} \left[\Phi_{21}(\zeta) + (\zeta - 1)^{\gamma_B} \Phi_{22}(\zeta)\right],$$

where Φ_{11}, Φ_{12}, Φ_{21}, Φ_{22} are analytic in the whole plane.

It implies that

$$f(\zeta) = \zeta^{\beta_C}(\zeta - 1)^{\beta_B}[\Phi_{11}(\zeta) + \zeta^{\gamma_C}\Phi_{21}(\zeta) + (\zeta - 1)^{\gamma_B}\Phi_{12}(\zeta) + \zeta^{\gamma_C}(\zeta - 1)^{\gamma_B}\Phi_{22}(\zeta)].$$

For definiteness we set (it is true for our problem) $-1 < \beta_C < -\frac{1}{2}, \quad -1 < \beta_B < -\frac{1}{2}$. According to *Property 3*, the right-hand part in the last equation sum must be representable as:

$$\Phi_{11}(\zeta) + \zeta^{\gamma_C}\Phi_{21}(\zeta) + (\zeta - 1)^{\gamma_B}\Phi_{12}(\zeta) + \zeta^{\gamma_C}(\zeta - 1)^{\gamma_B}\Phi_{22}(\zeta) = \Phi_\infty(\zeta)\zeta^\eta,$$

where $\eta = -1 - \beta_C - \beta_B, 0 < \eta < 1$ and $\Phi_\infty(\zeta)$ is an analytic function near infinity. Obviously, the analytic function $\Phi_{11}(\zeta)$ must tend to zero at infinity and due to the Liouville theorem $\Phi_{11}(\zeta) \equiv 0$. The points $\zeta = 0$ and $\zeta = 1$ are essentially singular and hence γ_C and γ_B are not integer. Therefore, the above expression is possible if $\gamma_C = \gamma_B = \eta$ and $\Phi_{22} \equiv 0$. Again, according to the Liouville theorem both Φ_{21} and Φ_{12} must be constants.

Thus, the function sought is:

$$f(\zeta) = \zeta^{\beta_C}(\zeta - 1)^{\beta_B}(D_1\zeta^\eta + D_2(\zeta - 1)^\eta), \tag{14}$$

where D_1 and D_2 are complex constants according to *Property 2*.

3.3. Determination of the free surface

Since the angles of G_z at points B and C are ν_B and ν_C, we can write:

$$\beta_B = \nu_C - 1, \qquad \beta_C = \nu_B - 1.$$

We determine two complex constants D_1, D_2 in (14) from the geometry of our flow domain. Since AB and AC are straight lines with an angle of inclination $\pi\mu$, we have

$$D_1 = -C_1 e^{i\pi\mu}, \qquad D_2 = -C_2 e^{i\pi\mu},$$

where C_1 and C_2 are two real constants. From the jump condition of the functions $Z(\zeta)$ and $z(\zeta)$ in the vicinity of A we can establish that $C_1 + C_2 = d/\pi$. Finally, we get:

$$Z(\zeta) = \frac{1}{\zeta^{1-\nu_C}(1-\zeta)^{1-\nu_B}}\left[C_1 e^{i\pi(\mu+\nu_B)}\zeta^\eta - C_2 e^{i\pi(\mu-\nu_C)}(1-\zeta)^\eta\right],$$

where $\eta = 1 - \nu_B - \nu_C$.

To find the constants C_1, C_2 in (15), we integrate it as

$$z(\zeta) = C_1\Phi_1(\zeta) + C_2\Phi_2(\zeta),$$

where $\Phi_1(\zeta), \Phi_2(\zeta)$ are 'linear' solutions (corresponding to straight free surfaces BC_d and BC_u shown in Figure 3a, bold lines).

We can consider C_1, C_2 as problem parameters. Then H, d are expressed linearly through C_1, C_2. Hence, C_1, C_2 are linearly dependent on H, d and we can write them in the following form

$$C_1 = \frac{1}{\pi}\left(A_1 d + B_1\frac{H}{\sin\mu}\right), \qquad C_2 = \frac{1}{\pi}\left(A_2 d + B_2\frac{H}{\sin\mu}\right), \tag{16}$$

where A_i, B_i ($i = 2$) are the coefficients to be found. Let the pair $d_{(1)}$, $H_{(1)}$ corresponds to the first linear solution with angle ν_B (line BC_d in Figure 3a). For this solution $C_2 = 0$. From the slab thickness at infinity $C_1 = d_{(1)}/\pi$, which is the jump condition for $z(\zeta)$ (recall that z has a logarithmic behaviour at infinity). Since BC_d is a straight line, we have $H_{(1)} = d_{(1)}(\cot\pi\nu_B + \cot\pi\mu)\sin\mu$. Similarly, for the second linear solution (Figure 3a, line BC_u) $C_1 = 0$, $C_2 = d_{(2)}/\pi$, $H_{(2)} = d_{(2)}(-\cot\pi\nu_C + \cot\pi\mu)\sin\mu$. Consequently, from these conditions A_2, B_2 satisfy the system

$$\begin{aligned} &A_2 + B_2(\cot\pi\nu_B + \cot\pi\mu) = 0 \qquad (\text{from} \quad C_2 = 0),\\ &A_2 + B_2(-\cot\pi\nu_C + \cot\pi\mu) = 1 \qquad \left(\text{from} \quad C_2 = \frac{d_{(2)}}{\pi}\right). \end{aligned} \tag{17}$$

From (17) we express A_2, B_2 (and analogously A_1, B_1), substitute them in (16) and obtain:

$$C_1 = d\frac{\cot\pi\nu_B + H_d/(\sin\pi\mu)}{\pi(\cot\pi\nu_B + \cot\pi\nu_C)}, \qquad C_2 = d\frac{\cot\pi\nu_C - H_d/(\sin\pi\mu)}{\pi(\cot\pi\nu_B + \cot\pi\nu_C)}, \tag{18}$$

where $H_d = H/d$. So, we found the constants in (15) just as in [16, p. 161].

Now we separate the real and imaginary parts in (15) as

$$\begin{aligned} \frac{\mathrm{d}x}{\mathrm{d}\xi} &= C_1\cos\pi(\mu+\nu_B)\xi^{-\nu_B}(1-\xi)^{\nu_b-1} - C_2\cos\pi(\mu-\nu_C)\xi^{\nu_C-1}(1-\xi)^{-\nu_C},\\ \frac{\mathrm{d}y}{\mathrm{d}\xi} &= C_1\sin\pi(\mu+\nu_B)\xi^{-\nu_B}(1-\xi)^{\nu_b-1} - C_2\sin\pi(\mu-\nu_C)\xi^{\nu_C-1}(1-\xi)^{-\nu_C}. \end{aligned} \tag{19}$$

We integrate (19), using:

$$\int_0^\xi \tau^{-\nu_B}(1-\tau)^{\nu_B-1}\,\mathrm{d}\tau = \frac{\xi^{1-\nu_B}}{1-\nu_B}{}_2F_1[1-\nu_B, 1-\nu_B; 2-\nu_B; \xi],$$

$$\int_0^\xi \tau^{\nu_C-1}(1-\tau)^{-\nu_C}\,\mathrm{d}\tau = \frac{\xi^{\nu_C}}{\nu_C}{}_2F_1[\nu_C, \nu_C; 1+\nu_C; \xi],$$

where ${}_2F_1$ is the hypergeometric function [19, pp. 555–566].

Since $x(1) = y(1) = 0$ (point B is the origin of coordinates) we determine two constants of integration and arrive at the following parametric equation of BC:

$$\begin{aligned} x(\xi) = {} & -C_1\cos\pi(\mu+\nu_B)\left[\frac{\pi}{\sin\pi\nu_B} - \frac{\xi^{1-\nu_B}{}_2F_1[1-\nu_B, 1-\nu_B; 2-\nu_B; \xi]}{1-\nu_B}\right] +\\ & C_2\cos\pi(\mu-\nu_C)\left[\frac{\pi}{\sin\pi\nu_C} - \frac{\xi^{\nu_C}{}_2F_1[\nu_C, \nu_C; 1+\nu_C; \xi]}{\nu_C}\right],\\ y(\xi) = {} & -C_1\sin\pi(\mu+\nu_B)\left[\frac{\pi}{\sin\pi\nu_B} - \frac{\xi^{1-\nu_B}{}_2F_1[1-\nu_B, 1-\nu_B; 2-\nu_B; \xi]}{1-\nu_B}\right] +\\ & C_2\sin\pi(\mu-\nu_C)\left[\frac{\pi}{\sin\pi\nu_C} - \frac{\xi^{\nu_C}{}_2F_1[\nu_C, \nu_C; 1+\nu_C; \xi]}{\nu_C}\right], \end{aligned} \tag{20}$$

where $0 \leq \xi \leq 1$.

If the physical and geometrical parameters in (18) give $C_1 = 0$ or $C_2 = 0$, then the corresponding free surfaces are straight lines BC_d and BC_u (bold lines in Figure 3a). In these cases point M coincides with C or B, respectively, and the cut in G_w (Figure 4b) disappears. Factually, the general solution (20) is a linear combination of two 'straight-line solutions' and the curve BC is always located in the corresponding 'triangle' BC_dC_u (Figure 3a).

Of course, the head difference H can physically be higher than for two limiting straight-line regimes in Figure 3a. In this case, a seepage face appears and our solution is not valid. Hence, we can derive the restriction, which guaranties the regime without seepage faces:

$$-\cot \pi \nu_B < H_d \sin \pi \mu < \cot \pi \nu_C.$$

Since the hypergeometric function ${}_2F_1$ is a built-in procedure of modern computer algebra packages (*e.g.* [20, p. 750]) calculations in (20) were easily done. Figure 5a shows the free surface at $H_d = 0, \mu = \frac{1}{2}$. Figure 5b illustrates the case $\mu = 1/4, H_d = 0{\cdot}5$, curves 1–3 correspond to $R = 0{\cdot}1, 0{\cdot}2, 0{\cdot}3$. Figure 5c shows advancing phreatic surfaces at $\mu = 1/6$, $H_d = 1{\cdot}0$ for three rates $R = 0{\cdot}25, 0{\cdot}5, 0{\cdot}75$ (curves 1–3, respectively). From these graphs we can see that near the slopes the free surface (F_2F_3 in Figure 3b) is indeed close to a straight line as we assumed in our asymptotic analysis. However, between the pools its shape is non-trivial. For example, in Figure 5c at $R = 0{\cdot}5$ and $R = 0{\cdot}75$, the saturated zone near the point B 'overhangs' the dry zone, *i.e.*, a vertical line drawn from the upper pool and starting near B intersects the free surface twice! However, the 'overhanging' configuration is stable because pressure in the saturated zone is higher than atmospheric in the dry zone and therefore small disturbances on BC do not propagate. The 'cusp' near C in Figure 5c seems to be difficult to model by standard numerical codes and even in steady-state regimes the vicinity of corner points is scrutinized [21].

Let us compare our 2-D solution with the Boussinesq model [1, pp. 431–451], which assumes that the lines perpendicular to an impermeable bottom are equipotentials (so-called hydraulic approximation). As we have mentioned, in our potential model (5–8) the flow is nearly uniform sufficiently far from BC, *i.e.*, a remote streamline F_4F_5 in Figure 3a can be viewed as an inclined impermeable bottom. Let us introduce a longitudinal coordinate x_b oriented along this streamline (Figure 3c). According to the hydraulic model flow is one-dimensional from BF_4 to C_dF_5 and the phreatic surface $h_f(x_b, t)$ counted from F_4F_5 is no longer more a free surface in a mathematical sense. Instead, we have the following nonlinear diffusion-convection equation [22]:

$$\frac{\partial h_f}{\partial t} = \alpha \left[\sin \pi \mu \frac{\partial}{\partial x_b}\left(h_f \frac{\partial h_f}{\partial x_b}\right) + \cos \pi \mu \frac{\partial h_f}{\partial x_b} \right] \tag{21}$$

where $\alpha = k/m$.

Let us search for a solution of (21) in the form $h_f(x_b, t) = a(t)x_b + b(t)$. Substituting this expression in (21), we arrive at two ordinary differential equations. From the first one $a'(t) = 0$ and hence $a = \text{ const.} = \tan \pi \gamma$. From the second ODE $b = \alpha(\sin \pi \mu \tan^2 \pi \gamma + \cos \pi \mu \tan \pi \gamma)t$. Consequently, we obtain a traveling-wave solution to (21). Clearly, this straight-line phreatic surface may exist if water rises in both reservoirs at a constant rate R_d. Since $h_f = R_d / \sin \pi \mu$ and $\nu_C = \gamma + \frac{1}{2}$, we obtain that the 'hydraulic' rate $R_d = \alpha \sin \pi \mu (\sin \pi \mu \cot^2 \pi \nu_c + \cos \pi \mu \cot \pi \nu_C)$, *i.e.*, it is the same as in the local analysis (see Figure 3b) for the full 2-D potential model. Thus, we have discovered another example (see

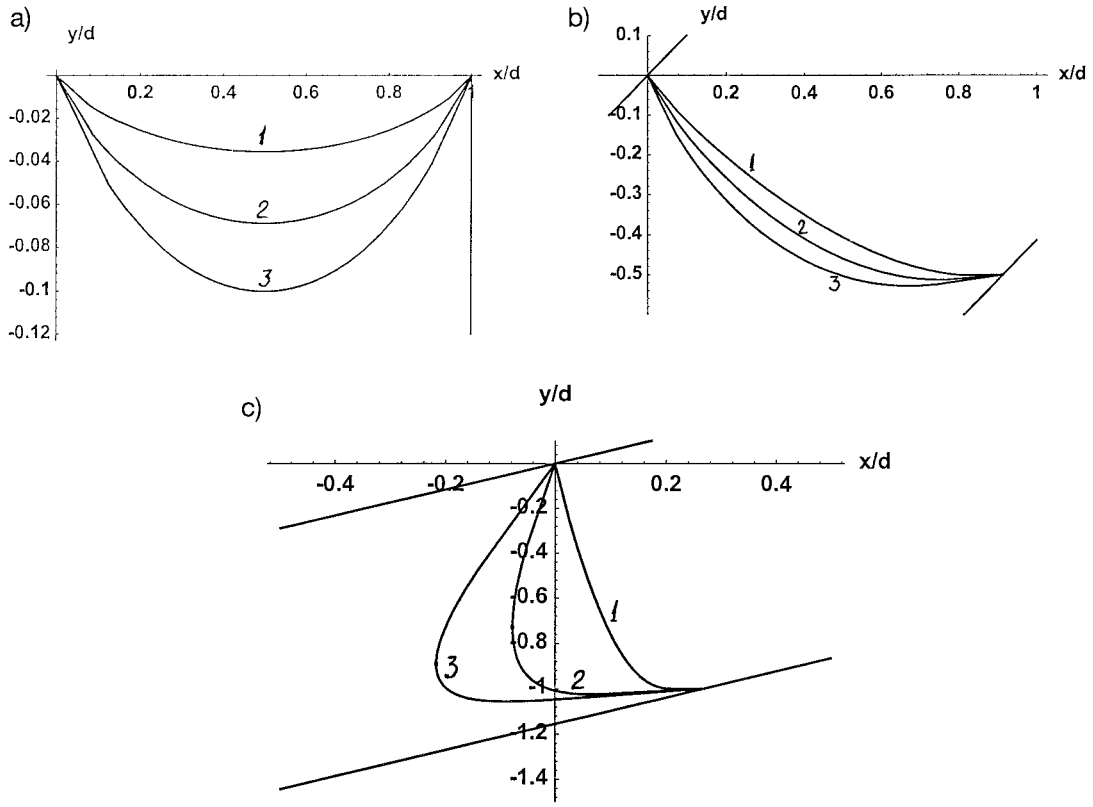

Figure 5. Free boundaries for various flow and geometric parameters.

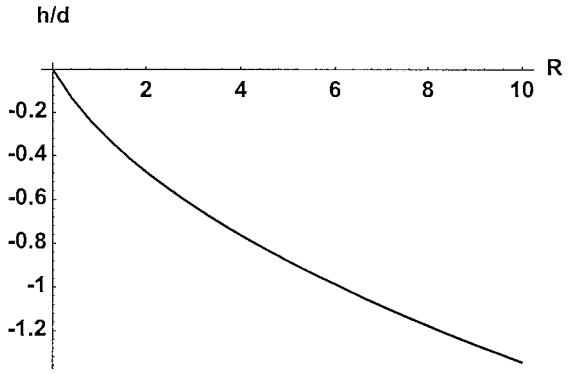

Figure 6. Nondimensional ordinate of the groove in Figure 2b ($H = 0$, $\mu = \frac{1}{2}$) as a function of R.

also [23], [24]) when straight-line solutions in hydrodynamic and hydraulic models match. Obviously, (21) as a one-dimensional model is unable to describe intricate flow patterns with a nonmonotonic phreatic surface or a hinge point as in Figure 3a.

In the simplest case $\mu = \frac{1}{2}$, $H = 0$ (Figure 2b) the curve BC is symmetric, $\nu_B = \nu_C = \nu = \pi^{-1}\text{arccot}\sqrt{R}$. The nondimensional ordinate of the deepest point $h = y(0{\cdot}5)/d$ (see Figure 2a) of the 'groove' as a function of R is shown in Figure 6 and illustrates the kinematic lag between the reservoirs' levels and the phreatic surface dragged behind. In this specific case, a water particle does not seep across the slab. Instead, pushed initially into the porous

medium by the rising reservoir levels, it decelerates with time and finally rests (at $\mu = \frac{1}{2}$ the velocity at point A is zero). Obviously, the Boussinesq model (21) at $\mu = \frac{1}{2}$ results in a trivial travelling-wave solution (with $\gamma = 0$). Hence, the Boussinesq model is not applicable in this case. Indeed, real seepage, as our potential model shows, is 'quasi-vertical', while the Dupuit–Forchheimer approximation postulates predominantly horizontal (parallel to the bed) flow, which does not exist, because there is no F_4F_3 streamline (Figure 3a) as in the general case $\mu \neq \frac{1}{2}$.

4. Discussion and conclusion

The Polubarinova–Kochina method to solve 2-D potential-flow problems with free surfaces is one of the most complicated to use in groundwater hydrology and geotechnical engineering. In the days when it was developed, the special functions in general and the Riemann symbolic representations of the derivatives of the complex potential and complex coordinate, which generally lead to hypergeometric functions, were difficult for a practical treatment. Even applied mathematicians, who encountered integration of these functions, had to rely on an asymptotic analysis and often only limiting cases of free-boundary problems were studied in full detail.

Modern symbolic software allows any engineer to check the old solutions from [1] or derive new ones (like those for our flow pattern with an advancing phreatic surface or mathematically similar steady-state seepage problems [15, 17, 25]). The solution presented is based on severe limitations. For example, we ignored the unsaturated zone, assumed a simple geometry of the flow domain (a strip-type layer) and a special flow regime (a constant rate of increase of water levels with not too high head drop across the slab). However, we used a rigorous 2-D potential model including on *a priori* unknown phreatic surface with two nonlinear (in terms of the velocity potential) boundary conditions [1, p. 548]. Therefore, the explicit and simple formulae derived may serve as tests for numerical codes applied to real problems with moving phreatic surfaces.

5. Acknowledgments

This study was supported by Sultan Qaboos University, projects AGSWAT 9903, AGR/99/13 and by the Russian Foundation of Basic Research, grants N99-01-00364, 99-01-00173. Helpful comments and criticism of four anonymous referees are appreciated.

References

1. P.Ya. Polubarinova-Kochina, *Theory of Ground Water Movement*. Moscow: Nauka (1977) (in Russian) 664 pp.
2. G. Kovacs, *Seepage Hydraulics*. Amsterdam: Elsevier(1981) 730 pp.
3. S.J. Lacy and J.H. Prevost, Flow through porous media: a procedure for locating the free surface. *Int. J. Num. Anal. Methods Geomech.* 11 (1987) 585–601.
4. B. Muhutham and C.L. Harwood, Seepage towards vertical cuts, *J. Geotech. Eng. ASCE* 115 (1989) 1339–1340.
5. M.E. Savci, Unsteady drawdown of water table. *J. Irrigation and Drainage ASCE* 116 (1990) 508–526.
6. A.R. Kacimov, Estimation and optimization of transient seepage with free surface. *J. Irrigation and Drainage ASCE* 119 (1993) 1014–1025.

7. I.L. Turner, B.P. Coates and R.I. Acworth, The effects of tides and waves on water-table elevations in coastal zones. *Hydrogeology J.* 4 (1996) 51–69.
8. G. Rehbinder, Relaxation of pore pressure in a slender core of a rockfill dam. *J. Hydraul. Res.* 35 (1997) 161–176.
9. P. Pelce, *Dynamics of Curved Fronts*. Boston: Academic Press (1988) 514 pp.
10. J. Crank, *Free and Moving Boundary Problems.* Oxford: Oxford University Press (1984) 425 pp.
11. J.F. Rodrigues, On the free boundary of the evolution dam problem. In: *Free Boundary Problems: Theory and Applications*, V.2. Boston: Pitman (1983) 125–134.
12. H.W. Alt, Nonsteady fluid flow through porous media. In: *Free Boundary Problems: Applications and Theory*, V.3. Boston: Pitman (1985) 222–228.
13. U. Hornung, Free and moving boundary problems arising in porous media flow and transport (rapporteur's report). In: *Free Boundary Problems: Theory and Applications*, V.1. New York: Longman (1990) 349–361.
14. H.R. Cedergren, *Seepage, Drainage and Flow Nets.* New York: Wiley (1989) 465 pp.
15. R.V. Craster, Two related free boundary problems. *IMA J. Appl. Math.* 52 (1994) 253–270.
16. S.D. Howison and J.R. King, Explicit solutions to six free-boundary problems in fluid flow and diffusion. *IMA J. Appl. Math.* 42 (1989) 155–175.
17. M. Bakker, Groundwater flow with free boundaries using the hodograph method. *Adv. Water Res.* 20 (1997) 207–216.
18. R.V. Craster and V.H. Hoang, Applications of Fuchsian differential equations to free boundary problems. *Proc. R. Soc. London A* 454 (1998) 1241–1252.
19. M. Abramovitz and I.A. Stegun, *Handbook of Mathematical Functions*. New York: Dover (1965) 1046 pp.
20. S. Wolfram, *The Mathematica*. Cambridge: Wolfram Media and Cambridge Univ. Press (1996) 1403 pp.
21. J. Aitchison, Numerical treatment of a singularity in a free boundary problem. *Proc. R. Soc. London A* 330 (1972) 573–580.
22. N.E.C. Verhoest and P.A. Troch, Some analytical solutions of the linearized Boussinesq equation with recharge for a sloping aquifer. *Water Resour. Res.* 39 (2000) 793–800.
23. A.R. Kacimov, Comment on the paper 'Linearised Boussinesq equation for modeling bank storage – a correction' by W.L. Hogarth, R.S. Govindaraju, J.Y. Parlange, J.K. Koelliker. *J. Hydrology* 218 (1999) 95–96.
24. A.R. Kacimov and Yu.V. Obnosov, Seepage in a near-reservoir saturated tongue controlled by evaporation from the phreatic surface. *Eur. J. Applied Math.* (submitted).
25. N.B. Ilyinsky, A.R. Kacimov and N.D. Yakimov, Designing the shape of soil slopes stable during seepage in Californian hillsides. R.J. Chandler (ed.), In: *Slope Stability Engineering. Proc. of the International Conf. on Slope Stability*. Londen: Thomas Telford (1991) pp. 67–70.